



Pulse radiolytic studies of supercritical CO₂¹

Nada M. Dimitrijevic^a, David M. Bartels^a, Charles D. Jonah^{a,*}, Kenji Takahashi^b

^a Chemistry Division, Argonne National Laboratory, Argonne, IL 60439, USA

^b Division of Quantum Energy Engineering, Hokkaido University, Sapporo 060, Japan

Received 22 February 1999; in final form 7 June 1999

Abstract

The species produced by ionizing radiation in supercritical CO₂ have been measured at a reduced temperature of 1.03 from 78 to 117 bar. It has been shown that C₂O₄⁺ is formed. This then reacts with positive ion scavengers. Its rate constant with dimethylaniline is $1.2 \times 10^{11} \text{ l mol}^{-1} \text{ s}^{-1}$ at 104 bar. The amount of C₂O₄⁺ formed is not proportional to the CO₂ density. This is attributed to an increased escape of the geminate ions at lower densities. We have also measured the production of ozone, which implies the production of O atoms and a production of oxygen molecules. Published by Elsevier Science B.V. All rights reserved.

1. Introduction

There are many motivations for the study of chemical reactions in supercritical fluids. Among these are the important technological uses that have been found for supercritical fluids and the even greater number of proposed uses of supercritical fluids, the interesting solvent properties existing in supercritical fluids, and the ability to alter the solvent properties over a wide range while not altering the molecular structure of the solvent or greatly altering the temperature or pressure.

There has been considerable effort in studying chemical reactions in supercritical fluids. Two recent

papers have reviewed these efforts and we will not attempt to recreate that discussion [1,2]. One facet of chemical reactions in supercritical fluids that does not appear to have been addressed is that of charged species and charge-transfer reactions in such solvents. The role of charge transfer can be very important in chemical reactivity.

Fast kinetic techniques often enable one to study the individual steps of chemical reactions. In these techniques, reactive species are created quickly and the evolution of these chemical species is observed. Flash photolytic techniques have been used by several research groups to study elementary radical reactions in supercritical fluids [3–5]. Recently pulse-radiolytic techniques have been applied to supercritical fluids [6–8]. Pulse radiolysis can access a different set of reactants than are normally created using flash photolysis. In particular, we are interested in the charge-transfer reactions. Radiolysis can easily create both positive and negative ions in a solution and these ions are well separated – not just an ion-pair.

* Corresponding author. Fax: +1 630 252 4993; e-mail: cdjonah@anl.gov

¹ Work performed under the auspices of the Office of Basic Energy Sciences, Division of Chemical Science, US–DOE under contract number W-31-109-ENG-38.

We recently have attempted to study electron-transfer reactions in supercritical fluids using pulse radiolysis [7,8]. The biphenyl anion was created in supercritical ethane and the rate of electron transfer from the biphenyl anion to the pyrene molecule was measured. We attempted to learn about the solvent reorganization energy by comparing the measured rates with the predicted rates using a diffusion-controlled reaction rate. Unfortunately, diffusion constants are not known in supercritical ethane and so all the conclusions were tentative.

We have now expanded our studies by measuring reactions in CO₂. The existence of a considerable quadrupole moment in the CO₂ molecule may greatly modify the solvent reorganization energy and thus the electron-transfer rate [9]. However, before beginning a series of studies of electron-transfer reactions in CO₂, it is necessary to understand the species formed and the reactions that occur in the neat supercritical fluids. Fortunately there has been considerable previous work done on the radiolysis of gaseous CO₂ [10–13]. Both the yields and kinetics of many species have been measured. These results have been used to create a kinetic model for radiolysis in gaseous CO₂ as a function of pressure.

In this preliminary report, we will show the existence of a positive ion and suggest its identity. We have measured the reaction rate of this cation with several species. In addition, we have observed the formation of ozone and suggest that it comes from the formation of oxygen atoms that are formed in the radiolysis.

2. Experimental

Experiments were run with a stainless-steel high-pressure cell with a 5 cm optical pathlength. The 1-cm-thick suprasil windows were mounted to the cell using Teflon o-rings. The temperature of the cell was maintained constant to $\pm 0.1^\circ\text{C}$ at 40.1°C (reduced temperature, $T_r = 1.03$) using an Omega temperature controller (Model CN1001RTD), a heater and a platinum resistance thermometer. The thermometer was installed into the cell so that it is in contact with the fluid. Pressures were generated using a JASCO HPLC pump (Model PU-980). The

fluid pressure was monitored with Cole-Parmer digital pressure meter (Model 7350-38) and pressure transmitter (Model K1, 3000 psi). Unless otherwise stated, all experiments were conducted at 104 bar total pressure. At this pressure and temperature the reduced density of CO₂ is 1.39 (density is 0.65 g cm^{-3}). The PVT relationships of CO₂ were calculated using the BWR equation [14].

The CO₂ was purchased from Scott Specialty Gases (SFC grade-diptube). When making samples using *N,N*-dimethylaniline the cell was purged with CO₂ for approximately 10 min. The purging flow was then sharply decreased and *N,N*-dimethylaniline was injected into the cell. The cell was then immediately closed and filled with CO₂ to the desired pressure. For gaseous additives, the system was evacuated before adding the solute gas. The pressure of the solute gas was measured and the system was pressurized with CO₂. It was necessary to pass the carbon monoxide (AGA, 99.993%) through a liquid nitrogen trap to remove impurities.

The experimental arrangement is similar to that which we have used previously [7,8]. To maximize the absorbance of the signal, the electron beam was colinear with the light beam. The light source was a 75 W xenon arc lamp that was pulsed for $300\ \mu\text{s}$ to increase the light intensity between 40- and 100-fold. Wavelength selection was done below 450 nm using a monochromator (PTI model 102). Above 410 nm, interference filters were used. (In the overlapping wavelength region, the technique depended on whether we were working from 410–1000 or 250–450 nm.) Light was detected in the UV–visible using a photomultiplier (Hamamatsu R928 with 5 dynodes in use); in the visible–near-infrared, an FND100 (EG&G) silicon photodiode was used. The signal from the detector was digitized using a Tektronix TDS 680B oscilloscope. All experiments except for the ozone production measurements used low dose pulses; the dose for the ozone measurements was 5–10 times bigger. Multiple irradiations of a single sample showed that there appeared to be no effect of irradiation on the measured data, except for the ozone production in the pure CO₂.

The radiation distribution in the cell was explored using Plexiglas (polymethylmethacrylate) absorption at 320 nm as a dosimeter [15] and measured using the thiocyanate dosimeter [16]. The pieces of Plexi-

glas were calibrated using the Fricke dosimeter [17]. The system was approximated by placing a window from the cell (1 cm thick) in the beam and four pieces of Plexiglas behind the window. The samples were contained in a beaker and experiments were made in the presence of water, hexane or air in the beaker. This allows us to determine how the density of the fluid will affect the dose distribution in the cell. For the 4 ns electron pulse, we obtained approximately 5.3 krad directly behind the window and about 5–10% of that value at the exit of the cell. The average dose for the 5 cm cell was approximately 2.75 krad for a 4 ns pulse. This value was approximately constant whether the beaker was filled with air, water, or hexane, showing that the dominant scattering is that of the front window. (Of course the actual energy deposited in the supercritical CO₂ will be proportional to its density. One rad is 100 erg of energy deposited per gram of material.)

The kinetic data were analyzed using a non-linear least-squares fitting routine, where the measured optical density is fit.

3. Results and discussion

3.1. Oxygen atom production

The transient spectrum and kinetics in neat CO₂ were measured from 250 to 350 nm. The strong UV spectrum of the final product is consistent with the literature spectrum of ozone [18]. The maximum concentration of ozone that is formed in a single pulse and a typical set of kinetic traces at 270 nm after different numbers of electron pulses is shown in Fig. 1. The product was found to be sufficiently stable so that its spectrum could be taken 30 min later using a conventional spectrophotometer.

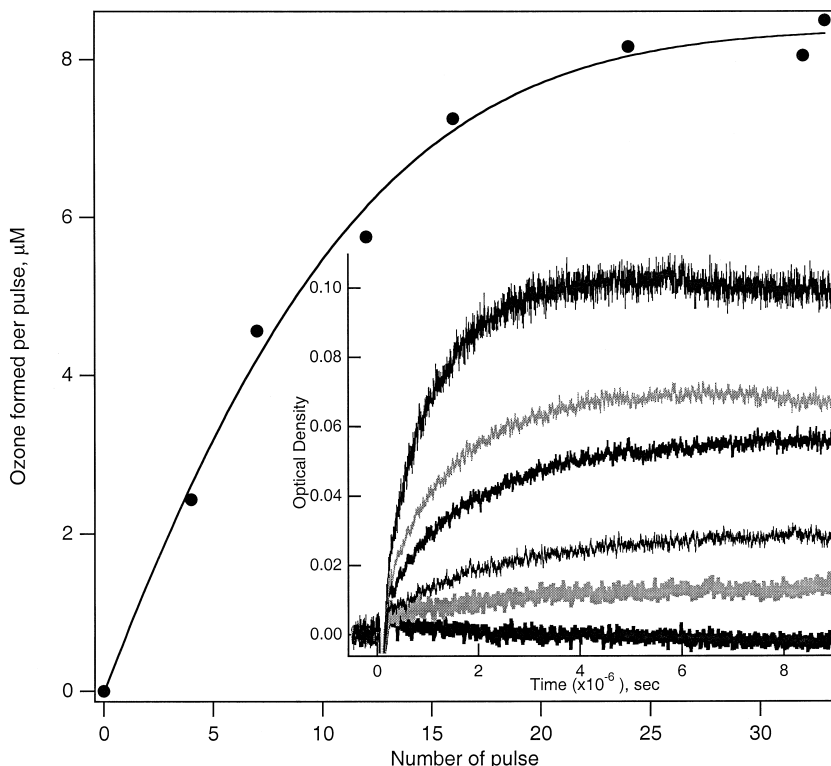


Fig. 1. Ozone production as a function of the number of pulses (10 krad/pulse) in pure CO₂ (104 bar). Inset shows the signal on the first, second, fourth, seventh, twelfth, and thirty-third pulse at 270 nm (first pulse the smallest and thirty-third the largest).

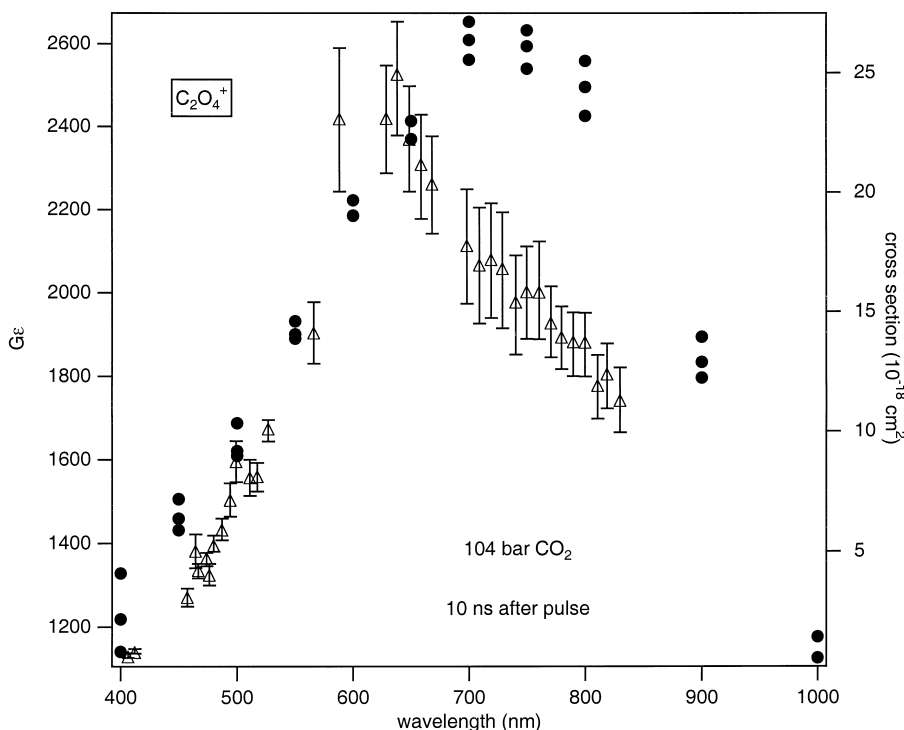
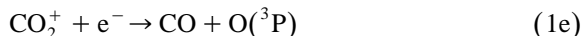
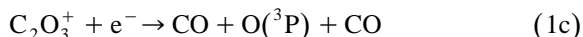
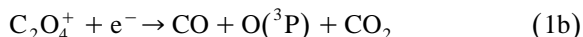


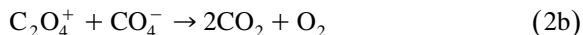
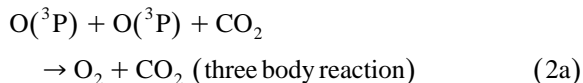
Fig. 2. Measured spectrum in irradiation of CO_2 at 104 bar and T_r of 1.03 (●) and cross-sections for photoionization from Ref. [24] (Δ). The left axis is in units of $G\varepsilon$ where G is the yield of C_2O_4^+ in molecules per 100 eV of energy deposited and ε is the absorption coefficient (base 10) in $\text{M}^{-1} \text{cm}^{-1}$ and the right axis is the photoionization cross-section.

From the work of Willis and Bindner [10] we can suggest the following set of reactions for the radiolysis of CO_2 .

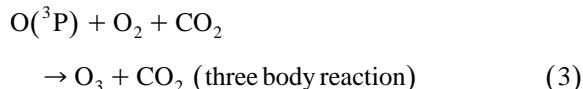
$\text{O}(^3\text{P})$ formation:



O_2 formation:



Ozone formation:



where $\text{O}(^3\text{P})$ is the ground-state oxygen atom (a triplet P-state). As the irradiation continues, molecular oxygen builds up in the cell (reaction (2a)). Direct production (1a) is expected to be the dominant source of $\text{O}(^3\text{P})$. Experiments with added SF_6 , which is known to react very fast with electrons [10], does not alter the kinetics. These results confirm the absence of an important ionic channel. The increase in oxygen molecules will then increase the rate at which reaction (3) occurs and thus increase the yield of ozone. This behavior is shown in Fig. 1. The presence of added CO does not alter the ozone yield.

We have determined a rate constant of $3 \times 10^{10} \text{ mol}^{-1} \text{ s}^{-1}$ at 104 bar for the $\text{O} + \text{O}_2$ reaction by

adding a low concentration of oxygen (20–100 μM) and measuring the rate of ozone formation after a single electron pulse. This reaction is a three-body reaction and thus the rate will depend on pressure, bath gas and temperature. Croce et al. measured the rate at 20°C in 60 atm CO_2 (below the supercritical pressure and temperature) and obtained a value of $9 \times 10^8 \text{ l mol}^{-1} \text{ s}^{-1}$ and estimated a limiting second order rate of $17 \times 10^8 \text{ l mol}^{-1} \text{ s}^{-1}$ [19]. The limiting rate was assumed to be the same for several bath gases. The same group has revisited the $\text{O} + \text{O}_2$ reaction and have shown that the limiting behavior will depend on the reaction mechanism [20].

3.2. Production of ions

One of the major processes in the radiolysis of CO_2 is expected to be the ionization of CO_2 to produce CO_2^+ and an electron. We know that CO_2 is an efficient electron scavenger in liquids [21], although the linear CO_2 molecule does not attach an electron efficiently in low-pressure gases [22]. With low concentrations of CO_2 in ethane, however, an equilibrium is created between a free electron and

CO_2^- [22]. It is known that the radical anion will transfer an electron to an aromatic solute both in polar [23] and non-polar solutions [21]. In previous experiments, we were unable to observe the formation of radical anions in CO_2 [7]. There are several explanations for this result. (1) We had not used SFC-grade CO_2 so it is possible that there were impurities in the gas that would react with the electron. (2) The anion of CO_2 might be part of a larger cluster and the electron affinity of the cluster might have been greater than that of the reactant. (3) The CO_2^- might fragment. The latter seems highly unlikely because this radical anion appears to be stable in hydrocarbons, in supercritical ethane and in water.

While we have not been able to explicitly follow the pathway of the negative ion, we have been able to determine the fate of the cation. In cluster experiments [24], the cation in CO_2 has been identified as C_2O_4^+ and its photodissociation (action) spectrum has been measured. Fig. 2 shows the spectrum that we observed in neat supercritical CO_2 within 10 ns of irradiation. Using the technique described above for measuring the dose, the absorption is given in units of $G\mathcal{E}$, where G is in units of molecules/100

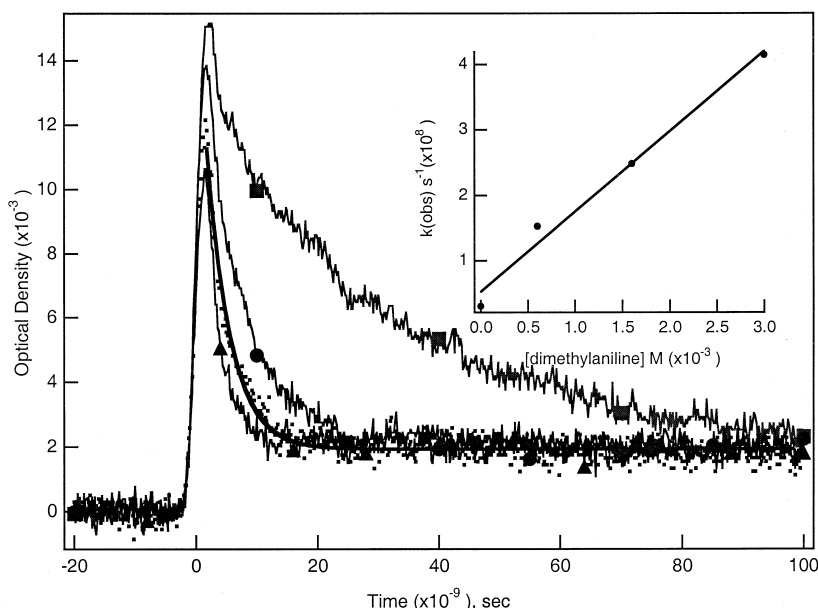


Fig. 3. Decay of absorption at 700 nm in 104 bar CO_2 with 0.0 (\blacksquare), 0.6 (\bullet), 1.6 (\cdot) and 3.0 (\blacktriangle) mM dimethylaniline added. The least-square fit is also shown for the 1.6 mM dimethylaniline (solid line). The inset shows the pseudo-first-order rate for dimethylaniline reaction with C_2O_4^+ as a function of dimethylaniline concentration.

eV of energy deposited and ε is the decadic extinction coefficient in units of $\text{cm}^2 \text{mol}^{-1}$. (Typical G -values are 1–5; much larger numbers would suggest a chain mechanism.) Also in this figure is the measured photodissociation spectrum of C_2O_4^+ [24]. One sees that the two spectra correspond quite well in the blue although the photodissociation spectrum drops much more sharply in the red. One might well expect this to be the case, if the quantum efficiency for photodissociation decreases at lower photon energies.

To further confirm the identity of the species that absorbs at 700 nm, we found that it reacted with water, oxygen and *N,N*-dimethylaniline (DMA) but not with SF_6 . Fig. 3 shows a typical trace for the reaction of DMA with the transiently formed species and the trace for the signal without DMA, as well as a non-linear least-square fit to the experimental data. By varying the concentration of DMA (see inset), the rate constant for the reaction of DMA was found to be $1.2 \times 10^{11} \text{ l mol}^{-1} \text{ s}^{-1}$ at 40.1°C and 104 bar. This rate is at or near the diffusion-controlled limit.

We also observed the products of the reaction with DMA in the 460 nm wavelength region. Unfortunately the cation spectrum of DMA is quite close to the spectrum of the triplet excited state, so we

could not cleanly isolate the kinetics of the cation formation [25]. We can see the formation of the triplet on a longer time scale. We expect that this comes about through the reaction of DMA^+ with an anion to form the triplet state.

In the presence of SF_6 the absorption at 700 nm increased, as shown in Fig. 4. SF_6 is known to be an electron scavenger and will react with some of the electrons that would otherwise geminately recombine with the cations (presumably the precursor of the C_2O_4^+ , the CO_2^+ molecule). This would then increase the yield of the C_2O_4^+ molecule. The decay of the cation appears to be faster in the presence of SF_6 but this may not be surprising. The reducing power of the electron has not been destroyed; it has just been altered by forming a lower mobility ion. Thus many of the reducing entities that would have decreased the initial yield, now react at longer times and contribute to the observed decay.

In radiolysis, ions and radicals are created by the interaction of the high-energy ionizing particle (electron or gamma) with the electrons of the molecules in the system. The number of ionizations is approximately proportional to the electron density and thus proportional to the density of the sample. When we measured the absorption of ozone (1 bar O_2 added) a

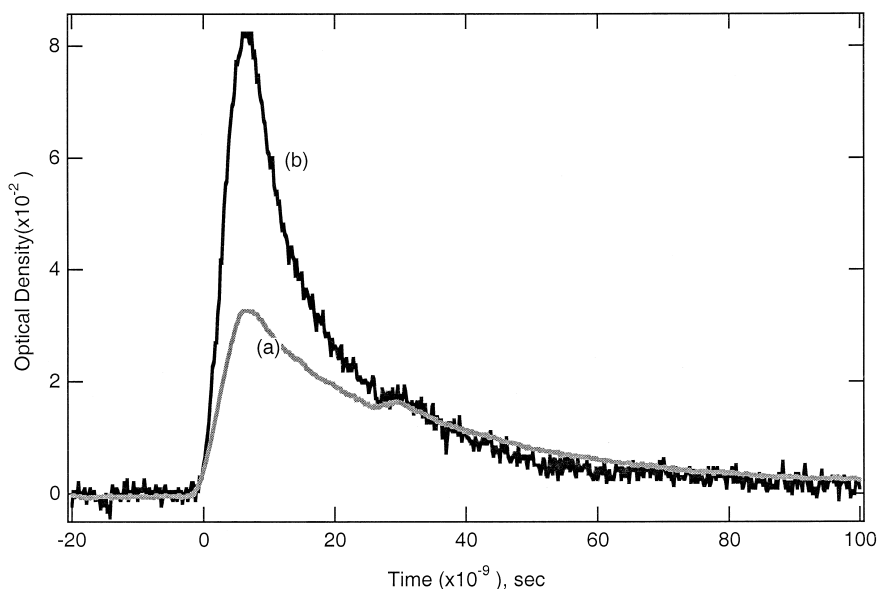


Fig. 4. Absorption measured at 700 nm at 104 bar in pure CO_2 (a) and in CO_2 with 0.04 M SF_6 (b). The step at approximately 25 ns is due to a small secondary pulse from the accelerator.

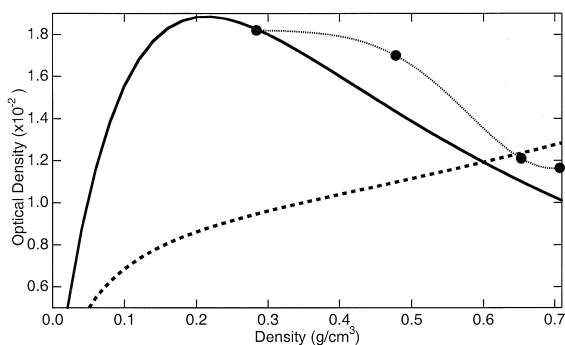
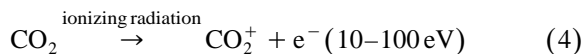


Fig. 5. The graph shows the maximum absorption of C_2O_4^+ as a function of density at 700 nm (●, line is to help guide the eye). Solid curve is the calculated yield assuming forward scattering of the electron, a separation of the positive and negative ion of 160 Å at a density of 0.6 g cm^{-3} and escape probability given by the Onsager relationship (see text for details). The dashed curve is a similar result for isotropic scattering.

linear dependence on density was found, indicating the amount of ozone formed was proportional to the energy deposited. However, as seen in Fig. 5, the amount of the C_2O_4^+ molecule formed is not proportional to the density; in fact the amount formed increases at lower density. One can describe the ionization process by the following equation:



where there is considerable energy in the electron that is ejected. This electron can then go a considerable distance in the fluid before it loses all of its energy and is thermalized. After it has lost its excess energy, its motion is diffusive and the electron will either geminately recombine with the cation or diffuse away. The probability of escape at a distance r , $P_{\text{esc}}(r)$ is described by the Onsager relationship [26],

$$P_{\text{esc}}(r) = e^{-r_0/r} \quad (5)$$

where r_0 is the distance where the coulomb attraction between the ions is equal to the thermal energy kT , which depends on the static dielectric constant. The thermalization distance will depend on density and the mechanism of electron scattering will determine the form of the density dependence. If the electron is forward scattered, the thermalization distance will be inversely proportional to density; if it is randomly scattered, the distance will vary as the inverse square root of the density. Different scatter-

ing modes will be important for different electron energies. Thus, given the thermalization distance at one density and the scattering mechanism, we can calculate the thermalization distance for other densities. We have plotted the predicted signal as a function of density along with the experimental data in Fig. 5. The distance distribution was derived assuming a thermalization distance of 160 Å at a density of 0.6 g cm^{-3} . As one can see, forward scattering with the selected thermalization distance can explain the general shape of yield versus density. We have not attempted to fit the data because one really expects a distribution of thermalization distances at each density and a mixture of forward and isotropic scattering.

4. Conclusions and future work

In this work we have shown that C_2O_4^+ is formed in the radiolysis of supercritical CO_2 and have measured its rate constants with dimethylaniline. We have also shown that ozone is formed by reaction between O_2 and ground-state oxygen atoms $\text{O}(^3\text{P})$ that are created in the radiolysis. The O_2 molecules are created through the recombination reactions of the $\text{O}(^3\text{P})$ atoms.

This work opens up many new experimental possibilities. We have begun measuring the rates of reaction between O_2 and C_2O_4^+ and dimethylaniline and C_2O_4^+ as a function of density. We expect that we can extract information from the density-dependent rate constants for these systems. In contrast to our studies in ethane, there seems to be considerable data available in the literature for diffusion constants in supercritical CO_2 so we expect the study of the density dependence of the electron-transfer reactions to be quite productive.

We also intend to measure the reaction rates for anions with aromatic molecules. It is to be hoped that from such data we will be able to learn about the roles of solvent fluctuations.

Acknowledgements

We would like to acknowledge Edwin Kemereit for operation of the accelerator and J.R. Miller for

use of data acquisition equipment. Acknowledgment is also made to the Office of Basic Energy Sciences, Division of Chemical Sciences of the Department of Energy for the support of Kenji Takahashi as a Visiting Scientist at Argonne National Laboratory. KT also acknowledges the Ministry of Education in Japan for Grant-in-Aid for Encouragement of Young Scientists.

References

- [1] B. Subramanian, M.A. McHugh, *Ind. Eng. Chem. Process Des. Dev.* 25 (1986) 1.
- [2] P.E. Savage, S. Gopalan, T.I. Mizan, C.J. Martino, E.E. Brock, *AIChE J.* 41 (1995) 1723.
- [3] C.B. Roberts, J.E. Chateauf, J.F. Brennecke, *J. Am. Chem. Soc.* 114 (1992) 8455.
- [4] C.B. Roberts, J. Zhang, J.F. Brennecke, J.E. Chateauf, *J. Phys. Chem.* 97 (1993) 5618.
- [5] C.B. Roberts, J. Zhang, J.E. Chateauf, J.F. Brennecke, *J. Am. Chem. Soc.* 115 (1993) 9576.
- [6] J. Zhang, K.A. Connery, J.F. Brennecke, J.E. Chateauf, *J. Phys. Chem.* 100 (1996) 12394.
- [7] K. Takahashi, C.D. Jonah, *Chem. Phys. Lett.* 264 (1997) 297.
- [8] K. Takahashi, S. Sawamura, C.D. Jonah, *J. Supercrit. Fluids* 13 (1998) 155.
- [9] L. Ebersson, *Adv. Phys. Chem.* 18 (1982) 79.
- [10] C. Willis, P.E. Bindner, *Can. J. Chem.* 48 (1970) 3463.
- [11] M. Yoshimura, M. Chosa, Y. Soma, M. Nishikawa, *J. Chem. Phys.* 57 (1972) 1626.
- [12] R. Kummeler, C. Leffert, K. Im, R. Piccirelli, L. Kevan, *J. Phys. Chem.* 81 (1977) 2451.
- [13] D.J. Norfolk, R.F. Skinner, W.J. Williams, *Radiat. Phys. Chem.* 21 (1983) 307.
- [14] H.W. Cooper, J.C. Goldfrank, *Hydrocarbon Process. Petrol. Refiner* 46 (1967) 141.
- [15] J.F. Fowler, F.H. Attix, *Solid state integrating dosimeters*, in: F.H. Attix, W.C. Roesch (Eds.), *Radiation Dosimetry-Instrumentation*, 2nd edn., vol. 2, Academic Press, New York, 1966, pp. 241–290.
- [16] R.H. Schuler, L.K. Patterson, E. Janata, *J. Phys. Chem.* 84 (1980) 2088.
- [17] H. Fricke, E.J. Hart, *Chemical dosimetry*, in: F.H. Attix, W.C. Roesch (Eds.), *Radiation Dosimetry-Instrumentation*, 2nd edn., vol. 2, Academic Press, New York, 1966, pp. 167–240.
- [18] M. Griggs, *J. Chem. Phys.* 49 (1968) 857.
- [19] A.E.C. de Cobos, J. Troe, *Int. J. Chem. Kinet.* 16 (1984) 1519.
- [20] H. Hippler, R. Rahn, J. Troe, *J. Chem. Phys.* 93 (1990) 6560.
- [21] M.C. Sauer, C.D. Jonah, *J. Phys. Chem.* 96 (1992) 5872.
- [22] M. Nishikawa, K. Itoh, R.A. Holroyd, *J. Phys. Chem. A* 103 (1999) 550.
- [23] A.J. Frank, M. Grätzel, A. Henglein, E. Janata, *Ber. Bunsenges. Phys. Chem.* 80 (1976) 294.
- [24] G.P. Smith, L.C. Lee, *J. Chem. Phys.* 69 (1978) 5393.
- [25] E. Zador, J.M. Warman, A. Hummel, *J. Chem. Soc., Faraday Trans. 1* 72 (1976) 1368.
- [26] C.H. Bamford, C.F.H. Tipper, R.G. Compton (Eds.), *Chemical Kinetics*, vol. 25, Elsevier, Amsterdam, 1985.